

# IMPROVING VIEWPOINT-INVARIANCE AND TEMPORAL CONSISTENCY FOR ACTION DETECTION

Yannick Porto<sup>\*†</sup> Renato Martins<sup>\*</sup> Thomas Chalumeau<sup>†</sup> Cedric Démonceaux<sup>\*</sup>

<sup>\*</sup> Université Bourgogne Europe, CNRS, ICB

<sup>†</sup> TEB Group, Prynél SAS

## ABSTRACT

Viewpoint change invariance and action temporal consistency are critical aspects for the effective deployment of human action detection of untrimmed videos. Existing appearance-based video detection methods often struggle with limited viewpoint diversity during training, while motion-based detection approaches frequently fail to model fine-grained temporal relationships across consecutive motion windows. This paper introduces a novel two-stage action detection approach designed to improve both view-invariance and global temporal coherence properties. In the first stage, we extract motion features from augmented virtual viewpoints, solely used at training. Then, the second stage introduces a new view-invariant, multi-scale temporal encoder based on selective state-space sequence modelling to aggregate information across viewpoints and time scales. Experiments on PKU-MMD and BABEL benchmarks demonstrate that this approach significantly outperforms state-of-the-art methods in all considered splits. Code and trained models are available at: <https://icb-vision-ai.github.io/HydraView-TAD>

**Index Terms**— Action Detection, Human Motion Analysis, Action Recognition.

## 1. INTRODUCTION

Temporal Action Detection (TAD) aims at recognizing and localizing human actions in long, untrimmed video sequences. Unlike trimmed action recognition, TAD requires not only identifying the action category but also accurately determining its temporal boundaries, making it a fundamental yet challenging problem for activity understanding. A critical aspect often overlooked in video-based methods is of explicitly considering viewpoint variability conditions. Changes in viewpoint can significantly alter the perceived action patterns, leading to inconsistencies in action representations and degraded detection performance. Beyond viewpoint changes, actions also typically exhibit strong temporal consistency across adjacent frames, where motion evolves smoothly over time. Local transitions provide essential cues for accurate boundary localization, and remains insufficiently addressed

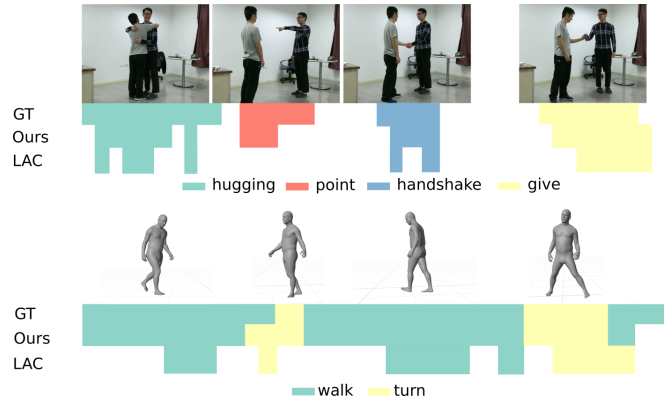


**Fig. 1.** Action detection on two sequences from PKU-MMD and BABEL datasets. GT indicates ground truth action labels per frame. Please notice the improved detection results from the proposed model (Ours) when compared to the baseline LAC for the actions “pointing” and “walk”.

by existing methods treating motion data. As a result, learning view-invariant representations that preserve temporal coherence across frames is essential for reliable TAD.

In this context, this paper proposes a novel multi-view TAD framework that jointly addresses view-invariance and temporal modeling in single-view sequences at inference. Our method decomposes untrimmed videos into small temporal windows and processes them in two main stages. First, we introduce a multi-view learning for window encoding with a new spatio-temporal encoder, suitable to reinforce temporal coherence in small periods of time. Compared to other skeleton-based action detectors [1, 2, 3], the spatial features are then frozen to train the temporal encoder. Learning relations on windows is costly, especially for long sequences, and moreover for multiple views. We therefore operate the same strategy than RGB-based TAD methods [4, 5, 6] with a two-step training.

Second, we propose a view-invariant multi-scale temporal encoder, termed HydraView, which aggregates information across both time and views to perform frame-level action detection, as illustrated in Fig. 1. HydraView is built upon a sequence of ViewMamba blocks that extend recent state

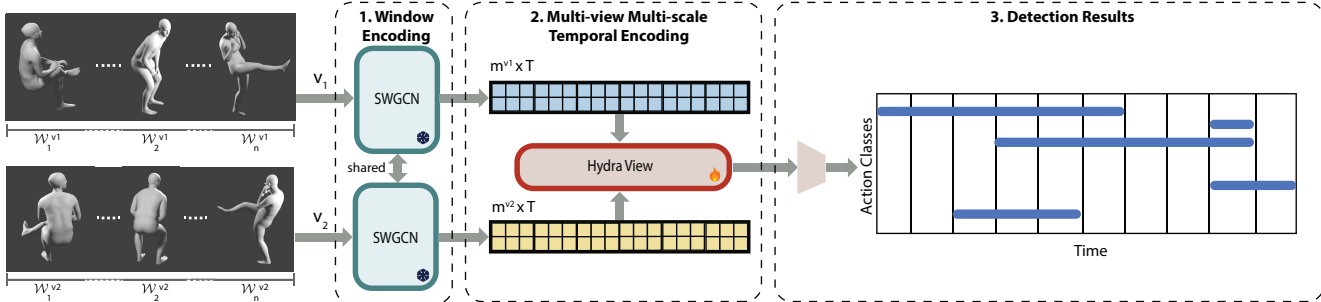


**Fig. 2.** Overview of our temporal action detection method with two viewpoints. For each input video viewpoint, an untrimmed sequence is encoded with a spatio-temporal encoder to generate features with improved view invariance. These features are then refined by our multi-view and multi-scale temporal encoder (HydraView) for localizing each action over time.

space model architectures to consider temporal and multi-view settings. Each block captures temporal relations at a specific scale while selectively scanning across both temporal and viewpoint dimensions. This design enables the model to handle simultaneously different viewpoints of the video at training and constrains the model to learn a similar action feature representation, reinforcing viewpoint-invariance. Then, a dedicated multi-scale fusion mechanism integrates these representations to produce accurate per-frame, multi-label action predictions.

Our method requires a set of different viewpoints solely at training time, and it is capable of considering at inference both single view and multi-view settings. Yet, to allow a fair comparison to competitors all results are shown in the context of a single viewpoint action detection. The main contributions of this paper are twofold: *i)* To the best of the authors’ knowledge, this is the first action detection model for learning temporal consistency on motion data captured across different viewpoints for the task of human temporal action detection. To achieve this, we transpose a two-stage training strategy commonly adopted in video-based action detection, enhanced with a multi-view motion encoding strategy, which is done solely at training time. *ii)* We introduce a new multi-view, multi-scale temporal architecture based on state space sequence modelling that jointly reasons over temporal dynamics and viewpoint variations with linear complexity in sequence length. The experiments show the capabilities of the designed approach, outperforming recent video and motion state-of-the-art temporal action detection methods on both PKU-MMD and BABEL benchmarks.

## 2. RELATED WORK

### 2.1. Video-based Action Detection

Early approaches to temporal action detection were largely proposal-based, drawing inspiration from object detection to generate candidate temporal segments. Although effective for sparsely annotated videos, these methods were computationally expensive and poorly suited for dense per-

frame predictions. To address these limitations, temporal convolution-based models were introduced to efficiently process long videos [4, 7, 8]. Such approaches, including Temporal Convolutional Networks, employ hierarchical temporal convolutions for fine-grained action detection [7], but their inherently local receptive fields restrict the modeling of long-range temporal dependencies [9]. More recently, transformer-based architectures have demonstrated strong performance in capturing both short- and long-term temporal dependencies [5], albeit at high computational cost due to quadratic attention complexity. To improve scalability, state space sequence models (SSMs) have emerged as efficient alternatives with linear complexity for long-sequence modeling [10, 11, 12, 13]. Several recent TAD methods integrate SSMs to balance expressiveness and efficiency [14, 15, 6]. In particular, CausalTAD [14], TimeMamba [15], and MS-Temba [6] explore different SSM-based designs for temporal action detection. Our approach builds upon these recent advances by leveraging multi-scale SSM operators, but considering a multi-viewpoint action recognition scheme.

### 2.2. Motion-based Action Detection

Several recent motion-based action detection approaches exploit auxiliary learning schemes to encode discriminative motion cues [1, 2], but they lack from temporal information since temporal features are globally pooled from all the sequence. Following this trend, [1, 2, 3, 16] focus on learning view-invariant skeleton representations at the frame level by training motion encoders on short temporal windows observed from varying viewpoints. Similarly to these works, we design a motion encoder to learn view-invariant representations with skeleton sequences observed from virtual viewpoints. These methods also refine per-frame features, but do not consider the relations between the different adjacent windows. In contrast, our proposed approach explicitly models local and long-range temporal dependencies at multiple scales, following strategies commonly adopted in video-based action features [4, 7, 17].

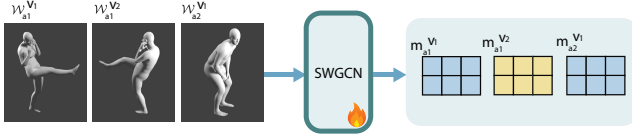


**Fig. 3.** Spatial feature encoding. Motion features are learned by small time windows for each viewpoint. The encoder model (SWGCN) is then frozen to extract window features with improved temporal consistency.

### 3. METHOD

This section presents the designed temporal action detection method to encapsulate properties from multiple viewpoints and long temporal sequences, as illustrated in Fig. 2. Following recent TAD methodologies [4, 7, 5], we start by pre-processing the input video sequence in small windows of time which are then encoded to learn relations along the whole video. Our methodology is composed of two main components: 1) A spatio-temporal motion encoding strategy to encode local windows of actions into spatially meaningful features, and 2) A new multi-view and multi-scale temporal feature encoder which learns the relations between the different windows over time and from the different viewpoints.

#### 3.1. Window Feature Motion Encoding

During training, we consider as input a 3D motion sequence which are divided into temporal windows. Each window  $\mathcal{W}$  in  $\mathbb{R}^{F \times J \times 3}$  consists of  $F$  frames with  $J$  body joints. The first step of our training scheme is to obtain projected 2D skeleton sequences, by simulating  $V$  virtual cameras with known parameters. As a result, each temporal window generates  $\mathcal{W}^v$  distinct 2D motion sequences inside  $V$  views. We simulate occlusions by masking limbs behind the torso joints. These projections provide diverse viewpoints and joint visibility patterns derived from a single underlying 3D motion. Following standard temporal action detection practices, each temporal window is composed of  $F = 16$  frames.

##### 3.1.1. Motion Feature Extraction

We start adopting a spatio-temporal graph convolution network [18] as in [19, 20, 21] to encode the features for small temporal windows. Spatio-temporal networks are designed for action recognition with larger windows of time (around 100 to 300 frames). When applied to short temporal windows, these design choices (temporal downsampling, batch normalization, or kernel size) can lead to a mismatch between the temporal receptive field and the available context, resulting in oversmoothing and reduced sensitivity to fine-grained motion cues. The specific architectural adaptations and tuned

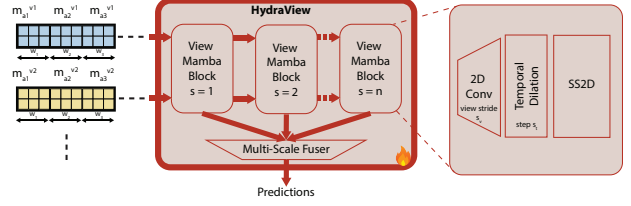


**Fig. 4.** Multi-view Multi-Scale Learning for Temporal Encoding with HydraView. HydraView is composed of multiple ViewMamba blocks each responsible of a specific scale in views and time. The ViewMamba block is a 2D convolution followed by a dilation module scaling the input for SS2D. The representation from each ViewMamba block is then processed by a Multi-Scale Fuser to provide the action predictions.

parameters used to address this issue are detailed in the supplementary material. We call this network Spatial-Window Graph Convolution Network (SWGCN) as depicted in Fig. 3.

Subsequently to refine and improve the temporal consistency of these initial features at window level, we adopt a two-stage encoding strategy, inspired by RGB-based temporal action detection methods. In the first stage, the spatial encoder is trained from scratch using the multiple  $\mathcal{W}^v$  observations as input. As illustrated in Fig. 3, a same action  $a1$  observed from two different viewpoints  $v1$  and  $v2$  is learned jointly and distinguished from a different action  $a2$ . During this stage, each temporal window is supervised with its corresponding action label using a cross-entropy loss. After convergence, the weights of the spatial encoder are frozen and window-level features are extracted into a vector  $\mathbf{M}^{vi} = [m_{a1}^{vi}, m_{a2}^{vi}, \dots]$  for the  $i^{th}$  view (left of Fig. 2).

#### 3.2. Multi-View and Scale Temporal Encoding

The proposed multiview action detection scheme requires the modelling of relations between the different views in the consecutive frames as well as the temporal consistency of actions in the whole sequence. For that, we propose HydraView (Fig. 4), a new network composed of multiple ViewMamba blocks, responsible of learning a unique representation from the temporal windows coming from all viewpoints. Building upon [6], each ViewMamba block is designed to model temporal dependencies at a specific scale, while explicitly adapting the architecture to the multi-view training regime.

##### 3.2.1. Scaling in ViewMamba

Each ViewMamba block depicted in Fig. 4 operates at a specific viewtemporal scale. Let  $\mathbf{M} \in \mathbb{R}^{V \times T \times C}$  denote the input multiview feature tensor, where  $V$ ,  $T$  and  $C$  are the numbers of views, temporal steps, and feature dimension respectively. The block begins with a 2D convolutional projection (Fig. 4) that applies a stride of  $s_v$  along the view dimension while

preserving the input temporal resolution. This view-strided convolution is defined as

$$\mathbf{M}_{k,t}^{(s_v)} = \sum_{i=0}^{K_v-1} \sum_{j=0}^{K_t-1} \mathbf{W}_{i,j} \mathbf{M}_{k s_v+i, t+j}, \quad (1)$$

where  $\mathbf{W} \in \mathbb{R}^{K_v \times K_t \times C}$  denotes the convolution kernel,  $K_v$  and  $K_t$  are the kernel sizes in the view and temporal dimensions, and  $(k, t)$  are the indexes of the output tokens. Following this convolutional projection, a temporal dilation operation is applied to increase the effective temporal receptive field. In particular, the convolutional responses are sampled with a dilation factor of  $s_t$  along the temporal dimension, such that temporal interactions are computed over indices spaced by  $s_t$ . This dilated temporal processing enables the ViewMamba block to model longer-range dynamics while operating on a reduced set of view-wise tokens.

### 3.2.2. Multi-View Temporal Scanning

Subsequently, the multiview modeling is performed with a selective state space model (SSM) inspired by Mamba and its 2D extension [10, 12]. Given an input sequence  $\mathbf{u}_t$ , derived from temporal dilation, the SSM dynamics are defined as:

$$\mathbf{h}_t = \mathbf{A}\mathbf{h}_{t-1} + \mathbf{B}\mathbf{u}_t, \quad (2)$$

$$\mathbf{y}_t = \mathbf{C}\mathbf{h}_t + \mathbf{D}\mathbf{u}_t, \quad (3)$$

where  $\mathbf{h}_t$  denotes the hidden state and  $\mathbf{y}_t$  the output at position  $t$ . In Mamba, the state transition parameters are input-dependent and computed through learnable projections:

$$\mathbf{B}_t = \mathbf{W}_B \mathbf{u}_t; \mathbf{C}_t = \mathbf{W}_C \mathbf{u}_t; \Delta t = \text{softplus}(\mathbf{W} \Delta \mathbf{u}_t), \quad (4)$$

with  $\mathbf{A}$  parameterized as a diagonal matrix,  $\mathbf{B}$ ,  $\mathbf{C}$  and  $\mathbf{D}$  the weighting parameters discretized using  $\Delta t$  [12]. This formulation enables efficient long-range dependency modeling while preserving linear-time complexity.

To jointly reason over temporal and view dimensions, the SSM scan is performed along four directions: (i) forward and backward along the view dimension, and (ii) left-to-right and right-to-left along the temporal dimension, as illustrated in Fig. 5. By introducing this adapted bidirectional 2D scanning, our model effectively retrieve relevant information across viewpoints while maintaining robustness to occlusions or missing detections over time.

We adopt a sequence of three ViewMamba blocks to process the sequence at different temporal scales. Concretely, each  $s^{th}$  block parses the sequence with a step of  $s$ , learning temporal relations between spaced frames. The different representations are then fused by a Multi-Scale Fuser: a VisionMamba [11] component applying a bi-directional horizontal scan to the multi-scale dimension before providing the final predicted actions. The designed HydraView is the key technical aspect of the method, providing most of the observed

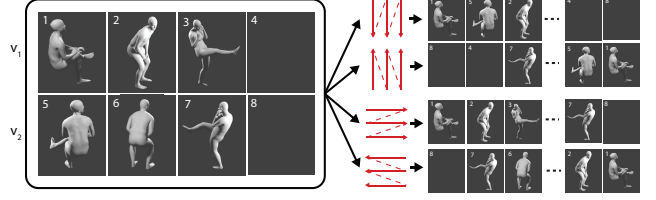


**Fig. 5.** Designed bidirectional scanning strategies along both view and temporal dimensions. This scheme shows actions seen from two viewpoints, and final empty cells mean a missing skeleton detection.

performance improvement, and consistently outperforms the state space modeling from MS-TEMBA [6] (as shown in the study on Tab. 3). In multi-label temporal action detection, each temporal segment indexed by  $t \in \{1, \dots, T\}$  may contain multiple action classes simultaneously. Therefore, this model is trained with independent binary cross-entropy (BCE) losses for each considered action classes per time step.

## 4. EXPERIMENTS

**Experimental Setup.** We train the motion encoder SWGCN with a feature dimension  $d = 384$ . The HydraView model responsible to enforce temporal coherence and viewpoint change invariance is composed of 3 ViewMamba blocks (each one in one scale), with an output dimension of 192 in each 2D convolution, a view stride of  $s_v = 2$  and a dilation rate of  $s_t = s$  for the  $s^{th}$  ViewMamba block. Each ViewMamba has state dimension 16. The number of virtual viewpoints at training was  $V = 12$ , with different body orientations spaced by  $30^\circ$ . The model optimization was done with AdamW, learning rate of 0.00045, and batch size 4. All experiments were done on an NVIDIA RTX 5000 Ada GPU.

**Datasets.** We have considered two widely-adopted public available action detection benchmarks (PKU-MMD and BABEL) for the evaluation. **PKU-MMDv1** [22] is an untrimmed video dataset containing 1076 sequences of around 4 minutes each. It has been recorded on three cameras positioned with a 45 angular separation between each. We consider the event-based mAP metric [1] for evaluation with a single view at inference as the competitors. Both evaluated cross-view (CV) and cross-subject (CS) splits involve viewpoint variations. **BABEL** [23] contains 43 hours of 3D human motion sequences from AMASS [24], annotated with over 63,000 frame-level labels across more than 250 action categories. We follow the exact experimental protocol adopted by (Yu and Fujiwara) [25] to build three subsets of actions.

**Baselines.** We have selected several relevant recent action detection methods for motion and video data, as shown in Tables 1 and 2. These competitors contain the current state-of-the-art approaches on each benchmark: LAC [1], USDRL [16], ASOT [26], SMQ [3] and S-WTAL [25].

**Table 1.** Detection mAP@IoU on PKU-MMDv1 cross-subject and cross-view splits.

Methods	CS		CV	
	10(%)	50(%)	10(%)	50(%)
JCRRNN[27] (ECCV'16)	45.2	32.5	–	–
Conv. Skel. [22] (MMW'17)	64.9	19.9	74.2	30.6
Skel. boxes [28] (ICMEW'17)	61.3	54.8	<u>94.5</u>	<u>94.2</u>
Hi-TRS [29] (ECCV'22)	–	67.3	–	–
LAC (scratch) [1] (ICCV'23)	<u>86.5</u>	74.6	92.9	90.1
USDRL [16] (AAAI'25)	–	<u>75.7</u>	–	–
Ours	<b>93.7</b>	<b>80.9</b>	<b>96.1</b>	<b>94.5</b>

**Table 2.** Detection mAP@IoU on BABEL subsets [25].

Method	Subset-1			Subset-2			Subset-3		
	10%	30%	50%	10%	30%	50%	10%	30%	50%
ASOT [26] (CVPR'24)	42.3	34.1	<u>24.5</u>	40.3	33.4	23.4	27.4	21.6	14.3
SMQ [3] (ICCV'25)	40.9	32.8	22.3	43.8	37.4	<u>27.4</u>	38.0	29.3	19.3
S-WTAL [25] (AAAI'23)	48.7	39.8	21.7	61.0	<u>50.3</u>	19.6	35.8	31.5	<u>20.4</u>
LAC [1] (ICCV'23)	<u>55.7</u>	<u>46.1</u>	24.2	<u>63.9</u>	48.5	26.7	<u>59.1</u>	<u>48.3</u>	20.2
Ours	<b>70.8</b>	<b>58.8</b>	<b>28.1</b>	<b>84.0</b>	<b>67.5</b>	<b>36.1</b>	<b>78.6</b>	<b>72.1</b>	<b>54.5</b>

#### 4.1. Detection Results

On PKU-MMD dataset shown in Tab. 1, our network achieves a mean Average Precision (mAP) exceeding 90% at IoU thresholds of 10% on both splits. Moreover, at an IOU of 50%, our network obtains a gain of +5.2% compared to the recent state-of-the-art USDRL [16] on this dataset. These findings can be also noticed in the provided qualitative results shown in Fig. 1. The detection improvement in comparison to LAC [1] is notably due to two aspects: actions such as “pointing” are better detected due to the view-invariant features. The improved temporal consistency of motion segments is also observed for actions such as “hugging” or “handshaking”, which enhances the mAP at a 50% IoU threshold.

These findings can also be observed for the results on the BABEL benchmark for all considered IoU thresholds (10%, 30% and 50%) as detailed in Tab. 2. Our method significantly outperforms the state-of-the-art results, yielding a +15% improvement across all subsets at 10% IoU and a +10% increase at 30 %IoU. Furthermore, the proposed approach also shows superior temporal consistency compared to existing methods, as it can be seen in the detection of “walk” actions in the sequences shown in Fig. 1. Please see the “Supplementary Material” for additional qualitative analysis.

#### 4.2. Ablation and Sensitivity Analysis

In designing our framework, we evaluated several spatial window encoders [19, 20, 21] commonly used in temporal action detection settings [1]. Table 3 reports the different combinations of window encoders (stage 1) and temporal encoders (stage 2) we investigated, along with the resulting performance on BABEL. Our approach consistently achieves mAP scores exceeding all evaluated window encoders, demonstrating that the proposed temporal encoder generalizes well across different backbone architectures. Furthermore, the

**Table 3.** Ablation and sensitivity on BABEL mAP@ 50%.

Window Encoder	Temporal Encoder	# views at train	Subset-1	Subset-2	Subset-3	
Different window encoders						(windows/sec)
PROTOGCN [21]	–	–	27.1	34.6	52.9	49
UNIK [20]	HydraView (Ours)	12	27.5	35.6	53.3	77
SWGCN (Ours)	–	–	28.1	36.1	54.5	115
Different temporal encoders						(sequences/sec)
–	–	–	22.3	24.9	50.1	–
SWGCN (Ours)	PDAN [4]	12	24.1	25.2	32.5	187
–	MS-TEMBA [6]	–	26.5	27.5	45.8	134
–	HydraView (Ours)	–	28.1	36.1	54.5	205
Different number of views						(sequences/sec)
–	–	1	24.7	30.2	48.2	–
SWGCN (Ours)	HydraView (Ours)	3	27.3	35.6	53.5	–
–	–	6	27.9	35.9	54.1	205
–	–	12	28.1	36.1	54.5	–

designed lightweight backbone (SWGCN), exhibits significantly faster inference compared to these alternative encoders, achieving nearly twice the speed of PROTOGCN [21].

The designed multi-scale temporal encoder (HydraView) also presents improved detection results when compared to the multi-scale strategies MS-TEMBA [6] and PDAN [4]. In addition, HydraView maintains competitive computational efficiency, processing up to 205 sequences per second. In this setting, each sequence consists of features extracted from 2,500 temporal windows that are subsequently refined by the temporal encoder. Furthermore, we analyze the behavior of our framework under varying numbers of generated virtual viewpoints at training time. This study reveals a consistent performance gain when multiple views are used compared to a single-view setting. Detection accuracy continues to improve as the number of views increases and begins to saturate when more than six viewpoints are incorporated.

## 5. CONCLUSION

This paper introduces a novel temporal action detection framework that jointly improves view invariance and temporal consistency. While existing video-based approaches generally lack robustness to viewpoint variations, motion-based detection methods often fail to model temporal relationships across adjacent windows. To overcome these limitations, we design a method based on two main components (SWGCN and HydraView) that leverages multiple viewpoints during training to enhance frame-level action localization in single-view untrimmed videos during inference. Our method combines multi-view learning on short temporal windows to enforce view-invariant yet discriminative motion representations with a multi-view, multi-scale temporal encoder based on recent state space models. The proposed approach achieves improvements over recent state-of-the-art temporal action detection methods on two widely adopted datasets PKU-MMD and BABEL.

**Acknowledgements.** This work was funded by TEB Group - Prynel SAS, and by grants ANER MOVIS from “Conseil Regional de Bourgogne-Franche-Comte” and ANR MANYVIS (ANR-23-CE23-0003-01), to whom we are grateful.

## 6. REFERENCES

- [1] Di Yang, Yaohui Wang, Antitza Dantcheva, Quan Kong, Lorenzo Garattoni, Gianpiero Francesca, and Francois Bremond, “Lac-latent action composition for skeleton-based action segmentation,” in *ICCV*, 2023.
- [2] Haitao Tian, “Duocl: Dual-surrogate contrastive learning for skeleton-based human action segmentation,” in *ICCV*, 2025.
- [3] Uzay Gökay, Federico Spurio, Dominik R Bach, and Juergen Gall, “Skeleton motion words for unsupervised skeleton-based temporal action segmentation,” in *ICCV*, 2025.
- [4] Rui Dai, Srijan Das, Luca Minciullo, Lorenzo Garattoni, Gianpiero Francesca, and François Bremond, “Pdan: Pyramid dilated attention network for action detection,” in *WACV*, 2021.
- [5] Yuhan Zhu, Guozhen Zhang, Jing Tan, Gangshan Wu, and Limin Wang, “Dual detrs for multi-label temporal action detection,” in *CVPR*, 2024.
- [6] Arkaprava Sinha, Monish Soundar Raj, Pu Wang, Ahmed Helmy, and Srijan Das, “Ms-temba: Multi-scale temporal mamba for efficient temporal action detection,” *CVPR*, 2026.
- [7] Rui Dai, Srijan Das, Kumara Kahatapitiya, Michael S Ryoo, and François Brémond, “Ms-tct: Multi-scale temporal con-  
vtransformer for action detection,” in *CVPR*, 2022.
- [8] Rui Dai, Srijan Das, Saurav Sharma, Luca Minciullo, Lorenzo Garattoni, Francois Bremond, and Gianpiero Francesca, “Toyota smarthome untrimmed: Real-world untrimmed videos for activity detection,” *TPAMI*, 2023.
- [9] Wen Wang, Xiaojiang Peng, Yu Qiao, and Jian Cheng, “An empirical study on temporal modeling for online action detection,” *CISIS*, 2022.
- [10] Albert Gu and Tri Dao, “Mamba: Linear-time sequence modeling with selective state spaces,” in *First conference on language modeling*, 2024.
- [11] Lianghui Zhu, Bencheng Liao, Qian Zhang, Xinlong Wang, Wenyu Liu, and Xinggang Wang, “Vision mamba: Efficient visual representation learning with bidirectional state space model,” in *ICML*, 2024.
- [12] Yue Liu, Yunjie Tian, Yuzhong Zhao, Hongtian Yu, Lingxi Xie, Yaowei Wang, Qixiang Ye, Jianbin Jiao, and Yunfan Liu, “Vmamba: Visual state space model,” *NeurIPS*, 2024.
- [13] Xiaoyong Lu and Songlin Du, “Jamma: Ultra-lightweight local feature matching with joint mamba,” in *CVPR*, 2025.
- [14] Shuming Liu, Lin Sui, Chen-Lin Zhang, Fangzhou Mu, Chen Zhao, and Bernard Ghanem, “Harnessing temporal causality for advanced temporal action detection,” *arXiv preprint arXiv:2407.17792*, 2024.
- [15] Guo Chen, Yifei Huang, Jilan Xu, Baoqi Pei, Zhe Chen, Zhiqi Li, Jiahao Wang, Kunchang Li, Tong Lu, and Limin Wang, “Video mamba suite: State space model as a versatile alternative for video understanding,” *IJCV*, 2026.
- [16] Wanjiang Weng, Hongsong Wang, Junbo Wang, Lei He, and Guosen Xie, “Usdrl: Unified skeleton-based dense representation learning with multi-grained feature decorrelation,” in *AAAI*, 2025.
- [17] Haitao Tian and Pierre Payeur, “Stitch, contrast, and segment: Learning a human action segmentation model using trimmed skeleton videos,” in *AAAI*, 2025, vol. 39.
- [18] Sijie Yan, Yuanjun Xiong, and Dahua Lin, “Spatial temporal graph convolutional networks for skeleton-based action recognition,” in *AAAI*, 2018.
- [19] Lei Shi, Yifan Zhang, Jian Cheng, and Hanqing Lu, “Two-stream adaptive graph convolutional networks for skeleton-based action recognition,” in *CVPR*, 2019.
- [20] Di Yang, Yaohui Wang, Antitza Dantcheva, Lorenzo Garattoni, Gianpiero Francesca, and Francois Bremond, “Unik: A unified framework for real-world skeleton-based action recognition,” *BMVC*, 2021.
- [21] Hongda Liu, Yunfan Liu, Min Ren, Hao Wang, Yunlong Wang, and Zhenan Sun, “Revealing key details to see differences: A novel prototypical perspective for skeleton-based action recognition,” in *CVPR*, 2025.
- [22] Liu Chunhui, Hu Yueyu, Li Yanghao, Song Sijie, and Liu Jiaying, “Pku-mmd: A large scale benchmark for continuous multi-modal human action understanding,” *ACM Multimedia workshop*, 2017.
- [23] Abhinanda R. Punnakkal, Arjun Chandrasekaran, Nikos Athanasiou, Alejandra Quiros-Ramirez, and Michael J. Black, “BABEL: Bodies, action and behavior with english labels,” in *CVPR*, June 2021.
- [24] Naureen Mahmood, Nima Ghorbani, Nikolaus F. Troje, Gerard Pons-Moll, and Michael J. Black, “AMASS: Archive of motion capture as surface shapes,” in *ICCV*, Oct. 2019.
- [25] Qing Yu and Kent Fujiwara, “Frame-level label refinement for skeleton-based weakly-supervised action recognition,” *AAAI*, Jun. 2023.
- [26] Ming Xu and Stephen Gould, “Temporally consistent unbalanced optimal transport for unsupervised action segmentation,” in *CVPR*, 2024.
- [27] Yanghao Li, Cuiling Lan, Junliang Xing, Wenjun Zeng, Chunfeng Yuan, and Jiaying Liu, “Online human action detection using joint classification-regression recurrent neural networks,” in *ECCV*. Springer, 2016.
- [28] Bo Li, Huahui Chen, Yucheng Chen, Yuchao Dai, and Mingyi He, “Skeleton boxes: Solving skeleton based action detection with a single deep convolutional neural network,” in *ICMEW*. IEEE, 2017.
- [29] Yuxiao Chen, Long Zhao, Jianbo Yuan, Yu Tian, Zhaoyang Xia, Shijie Geng, Ligong Han, and Dimitris N. Metaxas, “Hierarchically self-supervised transformer for human skeleton representation learning,” in *ECCV*, 2022.
- [30] Colin Lea, Michael D Flynn, Rene Vidal, Austin Reiter, and Gregory D Hager, “Temporal convolutional networks for action segmentation and detection,” in *CVPR*, 2017.

# [Supplementary Material] – Improving Viewpoint-Invariance and Temporal Consistency for Action Detection

In this supplementary material, we provide additional implementation details and experimental results to the main paper. Sec. A mainly discusses the rationale behind the SWGCN design and highlights its advantages over the baseline ST-GCN. Sec. B presents additional quantitative and qualitative experiments, specifically evaluating the models performance with multi-view inputs at inference time.

## A. IMPLEMENTATION DETAILS

### A.1. SWGCN

The proposed spatio-temporal backbone departs from the original ST-GCN [18] design in several key aspects to better accommodate short-window Temporal Action Detection (TAD), as listed in Tab. 4. ST-GCN was originally introduced for clip-level action classification and employs temporal downsampling and fixed kernel configurations to progressively increase the temporal receptive field over long sequences. While effective for classification, such temporal downsampling reduces frame-level resolution and can obscure fine-grained temporal boundaries, which are critical for precise action localization. In contrast, we remove temporal downsampling entirely, ensuring that the temporal resolution of the feature maps matches that of the input window, thereby preserving subtle motion cues and boundary information within short clips.

Furthermore, ST-GCN adopts a uniform temporal convolution kernel size across layers, implicitly assuming a fixed temporal scale for action modeling. This assumption is less suitable for TAD, where the relevant temporal context is strongly constrained by the window length [30]. We therefore adjust the temporal kernel size to explicitly control the temporal receptive field, aligning it with the short temporal extent of the input (e.g., 16 frames). This avoids excessive temporal smoothing and prevents the receptive field from exceeding the effective temporal support of the window, which would otherwise dilute discriminative motion patterns.

Finally, ST-GCN relies on Batch Normalization, which assumes sufficiently large and homogeneous mini-batches. In TAD settings, training is often performed with small batch sizes due to high temporal resolution and sliding-window sampling, making batch statistics noisy and unstable. To address this limitation, we replace Batch Normalization with Group Normalization, which normalizes features independently of the batch dimension. This modification leads to more stable optimization and improved feature consistency across windows, a property that is particularly important for dense temporal prediction tasks such as TAD.

**Table 4.** Comparison between the standard ST-GCN architecture and the proposed TAD-oriented spatio-temporal backbone (SWGCN).

Component	ST-GCN	SWGCN
Target task	Action classification	Temporal action detection
Input length	Long clips (e.g., 64–300)	Short windows (e.g., 16)
Temporal downsampling	Yes (stride > 1)	No (stride = 1)
Temporal kernel size	9	Adjusted to window length
Temporal receptive field	Progressively expanded	Explicitly controlled
Normalization	Batch Normalization	Group Normalization

**Table 5.** Inference with multiple views for inference on BABEL mAP@ 50%.

Method	# views at infer.	Subset-1	Subset-2	Subset-3	(sequences/sec)
Different number of views					
	1	28.1	36.1	54.5	200
Ours	3	28.5	37.3	55.7	153
	6	29.1	39.4	57.2	97
	12	30.1	40.7	57.6	50

### A.2. Occlusion Estimations

The occlusion estimation module, introduced in Sec. 3.1, simulates the 2D skeleton artifacts typical of varied camera perspectives. In real-world scenarios, joints positioned on the far side of the actor relative to the sensor often yield low-confidence scores and are subsequently filtered. To model this phenomenon, we approximate the human torso as a 3D reference plane. For each joint, we compute the intersection between this plane and the vector extending from the camera to the joint using standard line-plane intersection equations. A joint is flagged as occluded if this vector intersects the torso plane, effectively mimicking the self-occlusion observed in monocular 2D pose estimation.

### A.3. Fuser Component

The Multi-Scale Fuser is centered around a VisionMamba layer [11], chosen for its linear scaling and global receptive field. To harmonize features across different granularities, multi-scale inputs are first projected through a dense layer and stabilized via layer normalization. These refined features are then processed by the VisionMamba backbone with the final predictions generated by a dense MLP head.

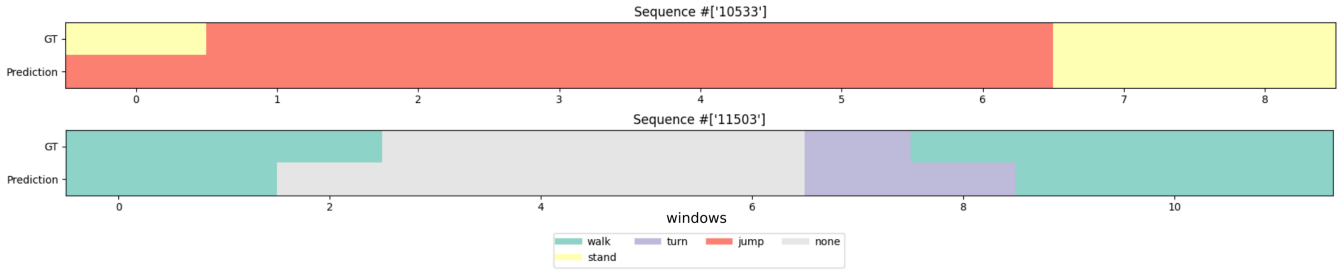


**Fig. 6. Results on two sequences from BABEL (split 1).** The predictions indicate the classification for each temporal window. Each action instance is correctly labeled. While some Detections exhibit minor temporal shifts at the boundaries, they maintain an Intersection over Union (IoU) exceeding 50%.

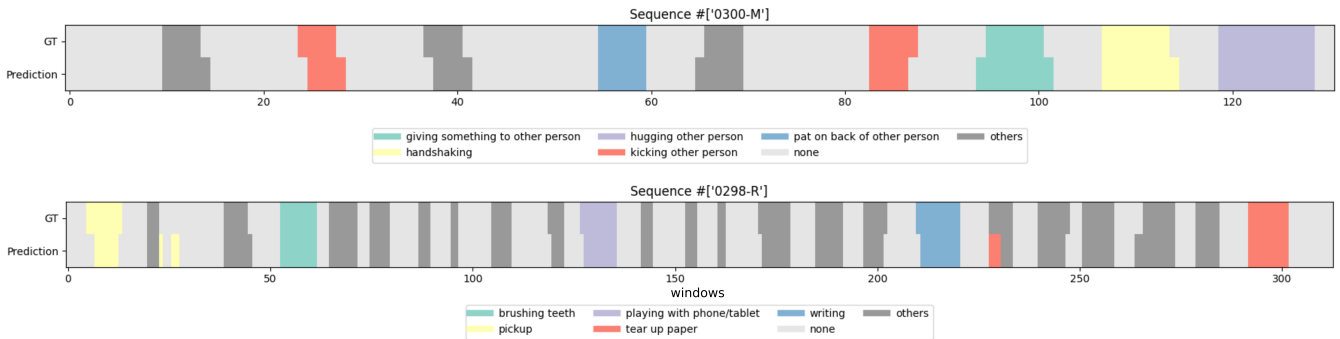


**Fig. 7. Results on two sequences from PKUMMDv1 (cross-subject split).** Our model effectively scales to long-form sequences (up to 4 minutes) involving a large action vocabulary (51 classes). For visual clarity, we aggregate “others” instances into a single category, though they retain their individual class labels for evaluation purposes. The results demonstrate the model’s ability to maintain temporal consistency across extended durations.

## B. FURTHER ANALYSIS

### B.1. Multi-view Inference

We also evaluate the performance of our end-to-end architecture across varying numbers of simultaneous views taken into account at inference as well (Tab. 5). This scenario is relevant if multiple video streams would be available such as on surveillance, CCTV or with camera rigs. Please notice however that all the previous results has been done considering a single view at inference for a fair comparison to the baselines (these results corresponds to 1 view row). Adding extra views at inference time brings supplementary information, therefore increasing the network accuracy. This demonstrates the ability of our network to aggregate features coming from different views at inference time as well. Even when considering 12 video streams at inference, our network achieves 50 sequences per second, contrasting favorably with existing temporal encoders that exhibit linear scaling complexity relative to the number of views. In this context, a single sequence comprises 2,500 temporal windows distributed across 12 views.

### B.2. Qualitative Results

This section provides additional qualitative visualizations to further evaluate the proposed framework. Fig. 6 illustrates the predicted action for each temporal window throughout the sequence. The observed temporal shifts between the ground truth (GT) and our predictions often stem from annotation ambiguity. Boundaries may vary based on whether an action is defined by the initial perceived motion or the physical displacement of joints. We also present qualitative results on the PKUMMDv1 dataset in Fig. 7. These longer sequences pose a significant challenge due to the density of action instances and the complex temporal dependencies between them. While our model accurately identifies most action boundaries, minor false detections remain, such as the “pickup” and “tear-up paper” instances in the bottom sequence, highlighting areas for future refinement.

### B.3. Per-Class Analysis

The per-class performance across the three BABEL splits demonstrates the model’s robust generalization capabilities, maintaining high Mean Average Precision (mAP) regardless

**Table 6.** Per-class analysis of our method on the different splits of BABEL, with an IoU of 10%.

BABEL split1	mAP	BABEL split2	mAP	BABEL split3	mAP
walk	84	sit	94	jog	79
stand	68	run	77	wave	68
turn	53	stand-up	89	dance	96
jump	79	kick	76	gesture	74

of the specific data partitioning. Notably, the model excels at identifying structured, periodic actions such as “dance” (96%) and “sit” (94%), suggesting that the temporal features of these classes are highly discriminative.

Conversely, more nuanced or transitional actions like “turn” (53%) and “stand” (68%) show relatively lower mAP scores. This likely stems from the inherent ambiguity in their start and end points, which pose a greater challenge for precise temporal localization (as observed in Fig. 6). Despite these variations, the results confirm that the model avoids complete misdetection of any single category, maintaining a performance floor above 50% across all evaluated splits. This consistency validates that the architecture is effectively capturing universal motion primitives rather than over-fitting to specific split distributions.